

## PAPER • OPEN ACCESS

Reaction Dynamics for the Systems  ${}^7\text{Be}$ ,  ${}^8\text{B}$  +  ${}^{208}\text{Pb}$  at Coulomb Barrier Energies

To cite this article: M Mazzocco *et al* 2018 *J. Phys.: Conf. Ser.* **1078** 012013

View the [article online](#) for updates and enhancements.

## Related content

- [8B + 208Pb Elastic Scattering at Coulomb Barrier Energies](#)

M. La Commara, M. Mazzocco, A. Boiano et al.

- [Scattering of the halo nucleus  \${}^{11}\text{Li}\$  and its core  \${}^9\text{Li}\$  on  \${}^{208}\text{Pb}\$  at energies around the Coulomb barrier](#)

M J G Borge, M Cubero, J P Fernández-García et al.

- [Strong reaction channels for the system  \${}^{17}\text{F} + {}^{58}\text{Ni}\$  at Coulomb barrier energies](#)

M Mazzocco, C Signorini, D Pierrousakou et al.



**IOP | ebooks™**

Bringing you innovative digital publishing with leading voices to create your essential collection of books in STEM research.

Start exploring the collection - download the first chapter of every title for free.

# Reaction Dynamics for the Systems ${}^7\text{Be}, {}^8\text{B} + {}^{208}\text{Pb}$ at Coulomb Barrier Energies

M Mazzocco<sup>1,2</sup>, A Boiano<sup>3</sup>, C Boiano<sup>4</sup>, M La Commara<sup>3,5</sup>, C Manea<sup>2</sup>,  
C Parascandolo<sup>3</sup>, D Pierroutsakou<sup>3</sup>, C Signorini<sup>6</sup>, E Strano<sup>1,2</sup>,  
D Torresi<sup>1,2,25</sup>, H Yamaguchi<sup>7</sup>, D Kahl<sup>7,26</sup>, L Acosta<sup>8,9,27</sup>, P Di Meo<sup>3</sup>,  
J P Fernandez-Garcia<sup>9,28</sup>, T Glodariu<sup>10,29</sup>, J Grebosz<sup>11</sup>,  
A Guglielmetti<sup>4,12</sup>, N Imai<sup>7,13</sup>, Y Hirayama<sup>13</sup>, H Ishiyama<sup>13</sup>,  
N Iwasa<sup>14</sup>, S C Jeong<sup>13,15</sup>, H M Jia<sup>16</sup>, N Keeley<sup>17</sup>, Y H Kim<sup>13</sup>,  
S Kimura<sup>13</sup>, S Kubono<sup>7,18</sup>, J A Lay<sup>1,2</sup>, C J Lin<sup>16</sup>,  
G Marquinez-Duran<sup>8</sup>, I Martel<sup>8</sup>, H Miyatake<sup>13</sup>, M Mukai<sup>13</sup>,  
T Nakao<sup>19</sup>, M Nicoletto<sup>2</sup>, A Pakou<sup>20</sup>, K Rusek<sup>21</sup>, Y Sakaguchi<sup>7</sup>,  
A M Sánchez-Benítez<sup>8</sup>, T Sava<sup>10</sup>, O Sgouros<sup>20,25</sup>, F Soramel<sup>1,2</sup>,  
V Soukeras<sup>20,25</sup>, E Stiliaris<sup>22</sup>, L Stroe<sup>10</sup>, T Teranishi<sup>23</sup>, N Toniolo<sup>6</sup>,  
Y Wakabayashi<sup>18</sup>, Y X Watanabe<sup>13</sup>, L Yang<sup>16</sup> and Y Y Yang<sup>24</sup>

<sup>1</sup> Dipartimento di Fisica e Astronomia, Università di Padova, Padova, Italy

<sup>2</sup> INFN-Sezione di Padova, Padova, Italy

<sup>3</sup> INFN-Sezione di Napoli, Napoli, Italy

<sup>4</sup> INFN-Sezione di Milano, Milano, Italy

<sup>5</sup> Dipartimento di Fisica, Università di Napoli "Federico II", Napoli, Italy

<sup>6</sup> INFN-Laboratori Nazionali di Legnaro (LNL), Legnaro (PD), Italy

<sup>7</sup> CNS - The University of Tokyo, RIKEN campus, Wako, Saitama, Japan

<sup>8</sup> Departamento de Física Aplicada, Universidad de Huelva, Huelva, Spain

<sup>9</sup> INFN-Sezione di Catania, Catania, Italy

<sup>10</sup> NIPNE, Magurele, Romania

<sup>11</sup> IFJ PAN, Krakow, Poland

<sup>12</sup> Dipartimento di Fisica, Università di Milano, Milano, Italy

<sup>13</sup> KEK, Tsukuba, Ibaraki, Japan

<sup>14</sup> Department of Physics, Sendai, Miyagi, Japan

<sup>15</sup> Institute for Basic Science, Daejeon, Korea

<sup>16</sup> China Institute of Atomic Energy, Beijing, China

<sup>17</sup> National Centre for Nuclear Research, Otwock, Poland

<sup>18</sup> RIKEN Nishina Center, Wako, Saitama, Japan

<sup>19</sup> Advanced Science Research Center, JAEA, Tokai, Ibaraki, Japan

<sup>20</sup> Department of Physics, University of Ioannina and HINP, Ioannina, Greece

<sup>21</sup> Heavy Ion Laboratory, University of Warsaw, Warsaw, Poland

<sup>22</sup> Department of Physics, University of Athens, Athens, Greece

<sup>23</sup> Department of Physics, Kyushu University, Hakozaki, Fukuoka, Japan

<sup>24</sup> Institute of Modern Physics, Chinese Academy of Sciences, Lanzhou, China

<sup>25</sup> Present address: INFN-Laboratori Nazionali del Sud (LNS), Catania, Italy.

<sup>26</sup> Present address: School of Physics and Astronomy, University of Edinburgh, Edinburgh, UK.

<sup>27</sup> Present address: Instituto de Física, Universidad Nacional Autónoma de México, Ciudad de México, Mexico.

<sup>28</sup> Present address: Departamento de Física Atómica, Molecular y Nuclear, Universidad de Sevilla, Sevilla, Spain.

<sup>29</sup> Deceased.



E-mail: marco.mazzocco@pd.infn.it

**Abstract.** In this contribution we describe the first results obtained for the investigation of the elastic scattering process in the reactions induced by the Radioactive Ion Beams  ${}^7\text{Be}$  and  ${}^8\text{B}$  on a  ${}^{208}\text{Pb}$  target at Coulomb barrier energies. The experimental data were analyzed within the framework of the optical model in order to extract the total reaction cross section. The comparison with data available in literature for reactions induced on  ${}^{208}\text{Pb}$  by light ions in the mass range  $A = 6-8$  shows that the loosely-bound  ${}^8\text{B}$  has the largest reactivity.

## 1. Introduction

The study of the reaction dynamics induced by light weakly-bound projectiles in the energy range around the Coulomb barrier has attracted the interest of the Nuclear Physics community since the early Nineties and the investigation was later boosted by growing availability of Radioactive Ion Beams (RIBs). Several review papers have been written on this topic in the past years [1, 2, 3, 4, 5, 6, 7].

These studies were originally aimed at measuring the sub-barrier fusion process. In fact, even in reactions induced by stable projectiles, a relevant enhancement of the fusion probability was observed at energies below the Coulomb barrier [8]. A detailed analysis showed that both static features, such as the nuclear deformation, and dynamical properties, such as the presence of transfer channels with positive  $Q_{value}$ , could dramatically alter the fusion cross section. With the advent of RIBs, it was expected that these effects could even be magnified by the unusual characteristics of these nuclei. In fact, especially in the lightest corner of nuclide chart we can find several examples of exotic nuclei with strong deformations or well established cluster configurations. Moreover, as a rather general feature, exotic projectiles are in most cases very loosely bound, with (total) binding energies often smaller than 1 MeV. It is therefore quite likely that, while approaching a target nucleus, a weakly bound projectile could more easily be broken by the interaction with the Coulomb and nuclear field provided by the reaction partner. We thus expect to observe large breakup cross sections, which should influence the whole reaction dynamics. From a theoretical point of view, if the breakup process is considered to be an additional open channel, we should quantum mechanically measure an enhancement of the sub-barrier fusion cross section. On the other side, if we treat the projectile breakup as a flux removal from the reaction input channel, then we might have a hindrance of the fusion probability, because we would have fewer particles at disposal for all other mechanisms.

Earlier measurements indicated a rather large increase of the sub-barrier fusion cross section [9], however it was soon realized that breakup related effects mostly enhanced the reaction rather than the fusion probability. This enhancement was mainly due to the 2n-stripping process, as for instance in  ${}^6\text{He}$ - [10, 11, 12] and  ${}^8\text{He}$ -induced [13, 14] reactions, whereas there are strong signatures that the breakup process could be responsible for the enhancement in reactions induced by the neutron-halo projectiles  ${}^{11}\text{Li}$  [15, 16] and  ${}^{11}\text{Be}$  [18, 17]. In all cases, serious deviations from the usual Rutherford scattering differential cross section were observed even at deep sub-barrier energies and this is another important evidence of strong reaction couplings.

Within this framework, we started the investigation of  ${}^7\text{Be}$ - and  ${}^8\text{B}$ -induced reactions.  ${}^8\text{B}$  is an extremely weakly-bound proton-halo nucleus ( $S_p = 0.1375$  MeV), while  ${}^7\text{Be}$  is the core of  ${}^8\text{B}$  and is a loosely-bound nucleus ( $S_\alpha = 1.586$  MeV) as well. As a difference with most of the RIBs studied so far, these two nuclei are located on proton rich side of the valley of  $\beta$ -stability and they might exhibit different features with respect to neutron halo and neutron skin nuclei. Until now, only the interaction of  ${}^7\text{Be}$  and  ${}^8\text{B}$  with light ( ${}^{28}\text{Si}$  [19, 20, 21]) and medium-mass ( ${}^{58}\text{Ni}$  [22, 23, 24]) has been investigated. Our study represents the first measurement performed at Coulomb barrier energies on the heavy target  ${}^{208}\text{Pb}$ .

## 2. Experiments

The  ${}^7\text{Be}$  RIB for this experiment was produced by using the EXOTIC facility [25, 26, 27] located at the Laboratori Nazionali di Legnaro (LNL) of the Istituto Nazionale di Fisica (INFN) in Legnaro, close to Padova (Italy). The experiment with the  ${}^8\text{B}$  was performed in Japan by means of the CNS Radioactive Ion Beam facility (CRIB) [28, 29] of the Center for Nuclear Studies (CNS) of The University of Tokyo and located inside the RIKEN campus in Wako-shi. In the next paragraphs we summarize the most important details concerning the RIB production and the experimental set-up employed for the two experiments.

### 2.1. ${}^7\text{Be}$ Experiment

*2.1.1. Beam Production* The  ${}^7\text{Be}$  delivered by the facility EXOTIC was produced employing the two-body reaction  $p({}^7\text{Li}, {}^7\text{Be})n$ , where a 48.8 MeV  ${}^7\text{Li}$  primary beam, accelerated by the LNL-XTU Tandem, was impinging on a gas target filled with 1 bar of hydrogen. The outgoing RIB was separated from the scattered beam and from the other contaminants up to a degree of purity of about 99% by using the eight ion optical elements of the facility. Details on the RIB production at EXOTIC can be found in the most recent publications [30, 31]. The secondary beam was impinging on a 1 mg/cm<sup>2</sup> thick  ${}^{208}\text{Pb}$  target foil with an intensity of  $2\text{--}3 \times 10^5$  pps. Three beam energies were obtained by operating the target station in different conditions (liquid nitrogen or room temperature) and inserting a aluminum degrader at a suitable position along the beam line. The beam energies at mid-target positions were: 37.4, 40.5 and 42.2 MeV.

*2.1.2. Experimental Set-up* Charge reaction products were detected with 6 modules of the detector array EXPADES [32, 33]. Each module consisted of a  $\Delta E$ - $E_{res}$  telescope of Double Sided Silicon Strip Detectors (DSSSDs). The thickness of the telescope inner ( $\Delta E$ ) and outer ( $E_{res}$ ) stage was 43-57 and 300  $\mu\text{m}$ , respectively. The active area of each DSSSD was 64 mm  $\times$  64 mm and was divided into 32 strips per side, thus allowing a 2 mm  $\times$  2 mm pixel resolution. The telescopes were placed symmetrically around the beam axis at the following mean polar angles:  $\theta_{lab} = \pm 69^\circ, \pm 111^\circ$  and  $\pm 153^\circ$  in order to cover approximately the angular  $\theta_{lab} = [50^\circ, 170^\circ]$ .

### 2.2. ${}^8\text{B}$ Experiment

*2.2.1. Beam Production* The  ${}^8\text{B}$  RIB for the experiment performed in Japan was produced by employing the inverse kinematics reaction  ${}^3\text{He}({}^6\text{Li}, {}^8\text{B})n$ , where the  ${}^6\text{Li}$  primary beam was delivered with an energy of 11 MeV/u by the RIKEN AVF Cyclotron and was hitting an 8-cm long gas cell inflated with  ${}^3\text{He}$  gas kept at liquid nitrogen temperature and at a pressure of about 1 bar. After the selection with the CRIB separator, the  ${}^8\text{B}$  beam was hitting a 2.2 mg/cm<sup>2</sup> thick  ${}^{208}\text{Pb}$  target with an intensity of  $10^4$  pps and a purity of about 20%. The secondary beam energy on target was about 50 MeV.

*2.2.2. Experimental Set-up* Also in this case, we employed six modules of the detector array EXPADES. However, in order to ensure a wider polar angle coverage, a slightly asymmetric arrangement was used. The mean polar angles of the six telescopes, in fact, were:  $\theta_{lab} = +27^\circ, \pm 69^\circ, \pm 111^\circ$  and  $-153^\circ$ , where the positive and negative signs preceding the polar angles indicate the left and right hemisphere (in a downstream view) of the scattering chamber. In such a way, it was possible to cover the angular range:  $\theta_{lab} = 15^\circ\text{--}165^\circ$ .

## 3. Preliminary Results

### 3.1. Elastic Scattering

Figures 1 and 2 show the preliminary evaluation of the elastic scattering angular distributions for the two reactions. Due to the secondary beam energy resolution and to the target thickness, it

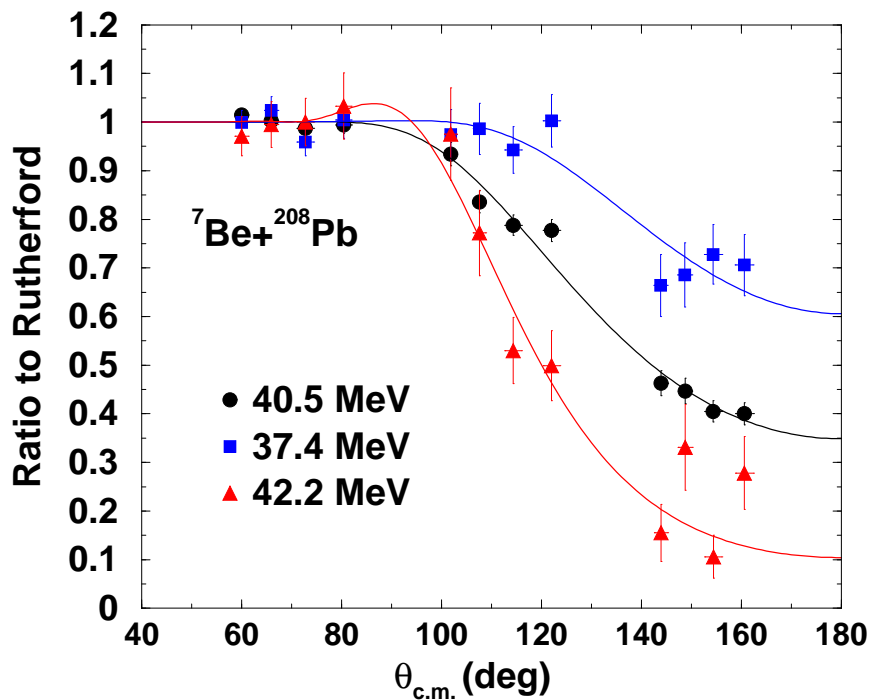


**Figure 1.** (Quasi-)elastic differential cross sections for the reaction  ${}^7\text{Be} + {}^{208}\text{Pb}$  at 37.4, 40.5 and 42.2 MeV. Continuous lines are optical model best-fits of the experimental data.

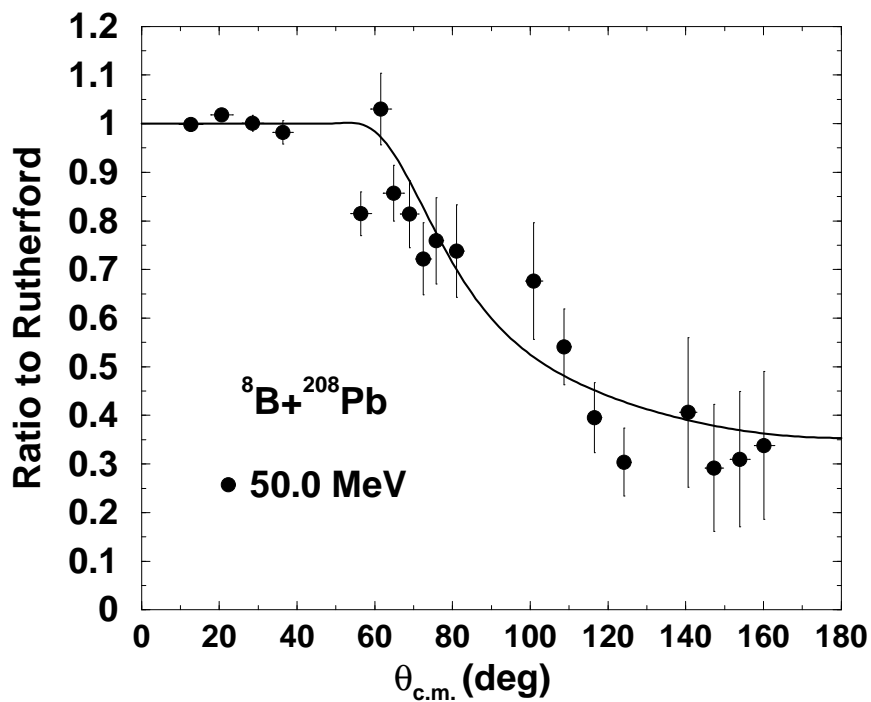


**Figure 2.** Elastic scattering differential cross section for the reaction  ${}^8\text{B} + {}^{208}\text{Pb}$  at 50 MeV. The continuous line is the result of the optical model best-fit analysis of the experimental data.

was not possible to solve experimentally pure elastic scattering events from inelastic excitations leading to the  ${}^7\text{Be}$  first excited state at  $E_x = 0.429$  MeV. For this reason, the experimental data displayed in Figure 1 have to be considered as quasi-elastic. To compensate the limited statistics gathered, the elastic scattering data were grouped into bins of four adjacent vertical strips and only four points per detector are represented in Figures 1 and 2. Where available, the average of the differential cross sections evaluated by telescopes located in the left and in the right hemisphere of the scattering chamber was considered.

The effects of the nuclear interaction between the projectiles and the target are clearly visible in both figures. The differential cross sections decrease as the scattering angles increases, since obviously the distance of closest approach decreases, and as the beam energy increases, as new reaction channels open up. The experimental data were fitted within the framework of the optical model in order to extract the total reaction cross section. The starting point of the fitting procedure was the Broglia-Winther parametrization [34] of the nuclear potential. The radius and diffuseness of both the real part and the imaginary part of the potential well were kept fixed and only the depths were let free to vary. The coupled channel code FRESKO [35] was employed for these calculations. Continuous lines in Figures 1 and 2 are the present results of the fitting procedure.

### 3.2. Reaction Cross Section

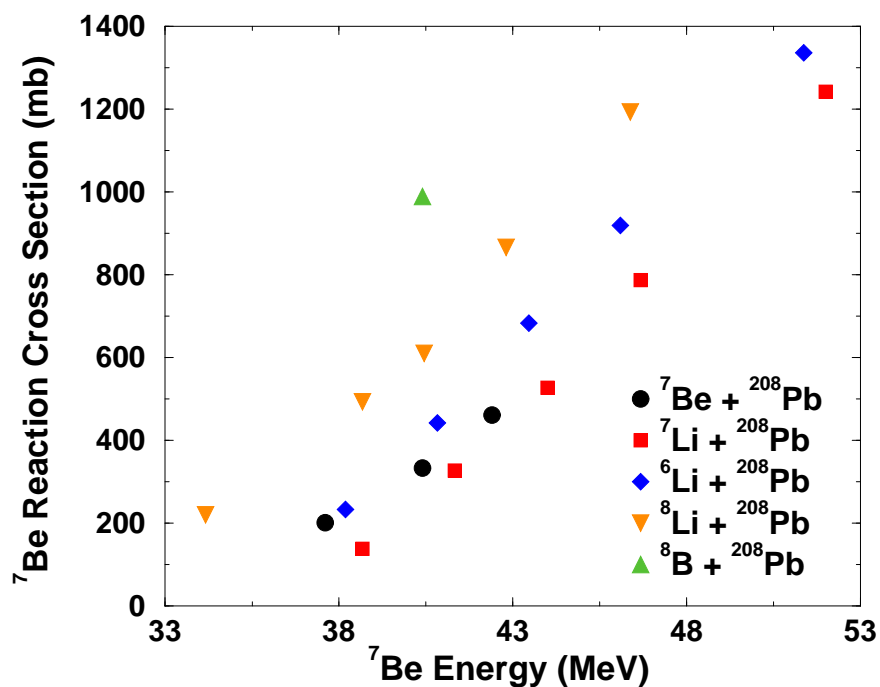


**Figure 3.** Preliminary evaluation of the total reaction cross sections for the systems  ${}^{6,7,8}\text{Li}$ ,  ${}^7\text{Be}$  and  ${}^8\text{B} + {}^{208}\text{Pb}$  at Coulomb barrier energies. To compare systems with different Coulomb barrier and geometrical size, energies and cross sections were normalized to the values for the system  ${}^7\text{Be} + {}^{208}\text{Pb}$ .

Figure 3 shows the comparison of the preliminary evaluation of the total reaction cross section for the three beam energies we measured for the system  ${}^7\text{Be} + {}^{208}\text{Pb}$  and the only energy point collected for the reaction  ${}^8\text{B} + {}^{208}\text{Pb}$ . For the sake of comparison, the total reaction cross

section data available in literature for the systems  ${}^{6,7,8}\text{Li} + {}^{208}\text{Pb}$  [36, 37] were also included in the figure. To account for the different Coulomb barrier and the different projectile size, the beam energies and the cross sections were normalized following the procedure described in [38] and then multiplied by the scaling factors for the system  ${}^7\text{Be} + {}^{208}\text{Pb}$ .

We can immediately appreciate that  ${}^7\text{Be}$  exhibits an intermediate behavior between that for  ${}^6\text{Li}$ , nucleus characterized by a very similar binding energy, and that for its mirror nucleus  ${}^7\text{Li}$ , which has a rather similar nuclear structure but is more bound by nearly 1 MeV. At near-barrier energies, where the projectile binding energy plays a major role, the total reaction cross section for the system  ${}^7\text{Be} + {}^{208}\text{Pb}$  resembles that for  ${}^6\text{Li}$ , whereas, as the beam energy increases, nuclear structure effects become more relevant and the  ${}^7\text{Be}$  reactivity approaches that for  ${}^7\text{Li}$ .

The comparison between the mirror nuclei  ${}^8\text{Li}$  and  ${}^8\text{B}$  is also very striking, being the reaction cross section for the boron isotope nearly twice that for the lithium counterpart. Such a large difference is presently interpreted as a direct consequence of the very small  ${}^8\text{B}$  binding energy and a possible signature of a strong breakup channel  ${}^8\text{B} \rightarrow {}^7\text{Be} + p$ .

#### 4. Perspectives

First-hand results on the reaction dynamics induced at Coulomb barrier energy by the two RIBs  ${}^7\text{Be}$  and  ${}^8\text{B}$  on a  ${}^{208}\text{Pb}$  target have been presented. The data analysis concentrated so far on the evaluation of the elastic scattering angular distributions in order to extract the total reaction cross sections. A preliminary comparison for the reactions induced at Coulomb barrier energies on a  ${}^{208}\text{Pb}$  target by light weakly-bound projectiles in the mass range  $A = 6-8$  has been presented.

The next steps of the analysis will consist in finalizing the theoretical calculations, by investigating, for instance, the relevance of inelastic excitations in the reaction induced  ${}^7\text{Be}$  and in producing reliable estimates for the breakup cross section in the system  ${}^8\text{B} + {}^{208}\text{Pb}$ . For an experimental point of view, the data analysis of the angular distributions for charged reaction products other than the projectile could provide additional insights on the reaction dynamics induced by these very exotic projectiles.

#### Acknowledgments

We all mourn our dear mate Tudor Glodariu, who unfortunately passed away on November 14<sup>th</sup>, 2017 at the age of 46. Tudor had been deeply involved in the lay-out and commissioning of the facility EXOTIC at INFN-LNL since the beginning of the project. He participated in all experiments performed, being in several cases the spokesperson or the co-spokesperson of the measurement. We will always remember his kind personality, his dedication to work, his fine sense of humor and the pleasure to have met in our lives a very special person like Tudor.

#### References

- [1] Canto L F, Gomes P R S, Donangelo R and Hussein M S 2006 *Phys. Rep.* **424** 1
- [2] Liang J F and Signorini c 2005 *Int. J. Mod. Phys. E* **14** 1121
- [3] Keeley N, Raabe R, Alamanos N and Sida J L 2007 *Prog. Part. Nucl. Phys.* **59** 579
- [4] Keeley N, Alamanos N, Kemper K W and Rusek K 2009 *Prog. Part. Nucl. Phys.* **63** 396
- [5] Mazzocco M 2010 *Int. J. Mod. Phys. E* **19** 977
- [6] Keeley N, Kemper K W and Rusek K 2014 *Eur. Phys. J. A* **50** 145
- [7] Canto L F, Gomes P R S, Donangelo R, Lubian J and Hussein M S 2015 *Phys. Rep.* **596** 1
- [8] Dasgupta M, Hinde D J, Rowley N and Stefanini A M 1998 *Ann. Rev. Nucl. Part. Sci.* **48** 401
- [9] Trotta M *et al* 2000 *Phys. Rev. Lett.* **84** 2342
- [10] A. Di Pietro A *et al* 2004 *Phys. Rev. C* **69** 044613
- [11] Navin A *et al* 2004 *Phys. Rev. C* **70** 044601
- [12] Raabe R *et al* 2004 *Nature* **431** 823
- [13] Lemasson A *et al* 2009 *Phys. Rev. Lett.* **103** 232701
- [14] Lemasson A *et al* 2010 *Phys. Rev. C* **82** 044617



- [15] Cubero M *et al* 2012 *Phys. Rev. Lett.* **109** 262701
- [16] Fernandez-Garcia J P *et al* 2013 *Phys. Rev. Lett.* **110** 142701
- [17] Pesudo V *et al* 2017 *Phys. Rev. Lett.* **118** 152502
- [18] Di Pietro A *et al* 2010 *Phys. Rev. Lett.* **105** 022701
- [19] Pakou A *et al* 2013 *Phys. Rev. C* **87** 014619
- [20] Sgouros O *et al* 2016 *Phys. Rev. C* **94** 044623
- [21] Sgouros O *et al* 2017 *Phys. Rev. C* **95** 054609
- [22] Aguilera E F *et al* 2009 *Phys. Rev. C* **79** 021601(R)
- [23] Aguilera E F *et al* 2011 *Phys. Rev. Lett.* **107** 092701
- [24] Mazzocco M *et al* 2015 *Phys. Rev. C* **92** 024615
- [25] Maidikov V Z *et al* 2004 *Nucl. Phys. A* **746** 389c
- [26] Pierroutsakou D *et al* 2007 *Eur. Phys. J. Spec. Top.* **150** 47
- [27] Farinon F *et al* 2008 *Nucl. Instrum. Meth. B* **266** 4097
- [28] Yanagisawa Y *et al* 2005 *Nucl. Instrum. Meth. A* **539** 74
- [29] Yamaguchi H *et al* 2008 *Nucl. Instrum. Meth. A* **589** 150
- [30] Mazzocco M *et al* 2008 *Nucl. Instrum. Meth. B* **266** 4665
- [31] Mazzocco M *et al* 2013 *Nucl. Instrum. Meth. B* **317** 223
- [32] Strano E *et al* 2013 *Nucl. Instrum. Meth. B* **317** 657
- [33] Pierroutsakou D *et al* 2016 *Nucl. Instrum. Meth. A* **834** 46
- [34] Broglia R A and Winther A 1981 *Heavy Ion Reactions* (Reading, MA: Benjamin)
- [35] Thompson I J 1988 *Comput. Phys. Rep.* **2** 167
- [36] Keeley N *et al.* 1994 *Nucl. Phys. A* **571** 32
- [37] Kolata J J *et al* 2002 *Phys. Rev. C* **65** 054616
- [38] Gomes P R S, Lubian J, Padron I, Anjos R M 2005 *Phys. Rev. C* **71** 017601